J Therm Anal Calorim (2010) 99:369–375
DOI 10.1007/s10973-009-0004-9

Thermal evolution of ceramic powders surrounding the $YBa_2Cu_3O_{7-x}$ composition

Edgardo R. Benavidez · Carlos J. R. González Oliver

Received: 3 February 2009 / Accepted: 7 May 2009 / Published online: 10 June 2009

Abstract Organometallic-derived ceramic compositions surrounding $YBa_2Cu_3O_{7-x}$ (123) were evaluated via DTA-TG runs and dilatometric densification. The compositions were either Y, Ba or Cu deficient respect to 123. For the Yttrium deficient compact the presence of liquids containing 0–1.3 mole $\%YO_{1.5}$—capable of dissolving the 123 grains—can promote a rapid sintering behavior. For Copper deficient compact the main densification/contraction mechanisms were delayed till 985 °C. For both Barium and Copper deficient compacts a strong exudation of liquids was detected at 990 °C and 1020 °C, respectively.

Keywords Dilatometry · Organometallic powder · Sintering · Superconductors · Thermal analysis

List of symbols

123	$YBa_2Cu_3O_7$
001	CuO
011	$BaCuO_2$
211	Y_2BaCuO_5
202	$Y_2Cu_2O_5$
$\Delta m/m_o$	Relative mass variation
m_o	Initial mass
$\Delta L/Lo$	[Lo-L(T)]/Lo: absolute shrinkage
Lo	Initial thickness of the pellet
L(T)	Instantaneous thickness of the sample at temperature T
$d(\Delta L/Lo)/dT$	Rate of linear shrinkage
ΔH_i	Enthalpy of reaction i

E. R. Benavidez (✉)
Facultad Regional San Nicolás, Universidad Tecnológica Nacional, B2900LWH San Nicolás, Argentina
e-mail: ebenavidez@frsn.utn.edu.ar

C. J. R. González Oliver
Centro Atómico Bariloche (CNEA), Av. Bustillo km.9.5, 8400 Bariloche, Argentina

C. J. R. González Oliver
C.O.N.I.C.E.T, Av. Rivadavia 1917, 1033 Buenos Aires, Argentina

Introduction

As it is known, the densification degree and the microstructure of ceramics influence most of the properties of a sintered material. Thus, in the $YBa_2Cu_3O_{7-x}$ (YBCO or 123) ceramic, the residual porosity and grain boundaries can alter significantly its superconducting properties [1]. For instance, YBCO materials with closed porosity exhibited broad and suppressed superconducting transitions [2]. This behavior was attributed to the difficulty in oxygenating these materials uniformly. However, this is not the only cause for degradation of the superconducting properties observed in high density materials prepared from carbon containing precursors: retention of C in the YBCO structure also causes a deleterious effect on the superconducting transition [3–6]. The detected fast densification formed closed pores, thus retaining the carbon incorporated in the system from the organic precursors.

In previous works YBCO organometallic solutions were used (a) for the deposition of superconducting films and (b) to produce -by gelation- fine powders of composition close to that for 123 [4, 7]. The chemical composition of the organometallic solutions was varied around 123 mainly to study (i) compound volatilization effects, (ii) possible reactions with particular ceramic substrates and (iii) formation of other phases than 123 that may help 123 to grow

in plate form. In such evaluations the partial pressure of O_2, the heating rate and the maximum temperature in the heat treatment were also varied. For instance, after deposition of 123 films on $SrTiO_3$ ceramic substrates it was found that the final composition of the film was deficient in Y and rich in Cu [7]. The crystal morphology consisted of needle/plate shaped grains with a little preferred orientation. This effect was attributed to a composition rich in $BaCuO_2$ (or to an oxycarbonate compound of $BaCuO_2$), which generated a liquid phase at around 900–920 °C (under O_2 flow) increasing significantly both the densification of the film and the crystal growth rate of platelets. The onset superconducting temperature (Tc) for such film was around 89 K, and the lowering in Tc (relative to 92 K for stochiometric 123) was attributed to carbon contamination of the 123-orthorhombic phase.

The whole dilatometric densification data for stoichiometric 123 pellets, obtained under constant heating rate (CHR) and isothermal (ISO) conditions, could be reasonably well explained in terms of existing solid state diffusion and liquid phase models [8]. It was also possible to propose that the densification of 123, in the important range between 922 °C and 970 °C in air (or 938–990 °C in O_2), is mainly controlled by the solution-precipitation model (SP) having a characteristic activation enthalpy of 207 kJ.mole^{-1} (229 kJ.mole^{-1} under oxygen flow). In a similar way the sintering behavior of Ag/123 laminates [9] was analyzed. The dilatometric technique was also found very useful to interpret the peritectic melting of 123, Ag/123 and $YBa_{(2-y)}$ $Sr_{(y)}$ Cu_3O_{7-x} compositions [10, 11]. Furthermore, from such studies interesting information about the properties of the different peritectic liquids associated to these different systems was obtained. Such liquids strongly control the growth of oriented plate-like grains in the 123 system during cooling from the peritectic range.

The aim of this work is to study the influence of chemical composition on the sintering kinetics of particular YBCO ceramics. The densification, the high temperature DTA (differential thermal analysis) and TG (thermogravimetric analysis) data of four powders of compositions close to and surrounding 123 are presented and analyzed. Such powders were obtained by gelation of organometallic solutions.

Experimental

Synthesis of powders and pellets

The organometallic solutions were obtained from (a) yttrium acetate [$Y(CH_3COO)_3 \cdot xH_2O$; Aldrich, 99.9%], (b) barium methoxyethoxide and (c) copper butyrate [$Cu(C_3H_7COO)_2$]. The Ba-methoxyethoxide was prepared by reacting pellets of barium metal (Aldrich, 99+%) with 2-methoxyethanol (Aldrich, 99.9%). The Cu compound was obtained by reacting $Cu(OH)_2$ with butyric acid ($CH_3CH_2CH_2CO_2H$; Riedel-de Haegen, 99%); the copper hydroxide was obtained by reacting $CuSO_4 \cdot 5H_2O$ (Timper, 99%) with NaOH (Brener, 99%). The (a, b and c) components were dissolved in suitable organic solvents and mixed together (according to individual calibrations after drying and calcining steps) to give compositions C0, C1, C2 and C3 (see Table 1). Each homogeneous liquid was poured into a beaker which was covered with Al-paper and let to gel and dry at 70 °C for 24 h. The dried powders had a strong green color and were subsequently calcined under O_2 flow at 890 °C for 12 h, and subjected to further oxidation at 460 °C for 6 h. After that, a black powder was obtained.

Polyvinyl butyral, (PVB, MW ~150,000, Polysciences, Inc.) was used as binder with a mass ratio PVB/powder = 0.02. The powder/PVB mixtures were pressed uniaxially at 100 MPa to form thin disks of 3.88 mm in diameter and 1.07–1.21 mm in height.

Prior to the dilatometric densifications, the pellets were slowly heated up to 750 °C, and maintained at that temperature for 4 h (under O_2 flow), attempting to eliminate the organic components. After such pre-firing treatment no shrinkage was detected in any compact.

Characterization techniques

The Neutron Activation Analysis (NAA) method (nuclear reactor RA-6, Centro Atómico Bariloche) was employed to measure the chemical compositions of the samples; this method was employed owing to the small quantities of powders available. Through this technique the γ-radiation emitted by the sample after irradiation with neutrons is measured. The energy and half-life time ($T_{1/2}$) are characteristics of each isotope of a given chemical element, and, the number of γ rays is proportional to the quantity of the element present in the sample. The analyzed isotopes were: Cu-66 ($T_{1/2}$ = 5.1 min, γ = 1039 keV), Ba-139 ($T_{1/2}$ = 83.06 min, γ = 1421 keV) and Y-90 m ($T_{1/2}$ = 3.19 h, γ = 480 keV).

Table 1 Chemical compositions and cationic ratios of the specimens

Powder	Wt%			Cation ratio
	$YO_{1.5}$	BaO	CuO	Y:Ba:Cu
C1	12.7	47.0	40.3	0.7:2.0:3.3
C2	18.7	41.1	40.2	1.1:1.7:3.2
C3	17.6	49.4	33.0	1.1:2.2:2.8
C0	17.1	46.2	36.7	1.0:2.0:3.0

The standards used were: metallic copper (Reactor Experiments Inc, 99.998%), $BaCO_3$ (Johnson Matthey, 99.997%) and $Y(NO_3)_3.4H_2O$ (Aldrich, 99.99%).

The crystalline phases were identified from X-rays diffraction (XRD) patterns obtained with a Philips PW 1700 diffractometer using as wavelength $\lambda_{Cu\ K\alpha} = 0.154054$ nm.

Simultaneous DTA and TG runs were performed using a Netzsch STA-409 apparatus at a heating rate of 10 °C.min^{-1} (up to 1070 °C) under O_2 flow. Sintered alumina crucibles and kaolin powder as the reference were used. After the DTA-TG runs up to 1,070 °C there was no indication of sample contamination by reaction with the alumina crucible.

The linear densification data, obtained under similar heating rates and atmosphere to those employed in the DTA-TG runs, were collected with a differential vertical dilatometer (Theta Dilatronics II); the push rod exerted a 10 kPa pressure on the specimen.

Results and discussion

Chemical composition and crystalline phases of the powders

Table 1 lists the mass percentages of the constituent oxides and the cation ratios after the NAA performed on the powders.

The measured compositions by NAA are plotted in Fig. 1 and it is noted that 123 composition (C0) is reasonably well surrounded by the different compositions.

The XRD data for such calcined powders are shown in Fig. 2. The crystalline phases found in these specimens are listed in Table 2. The codes and compositions of such

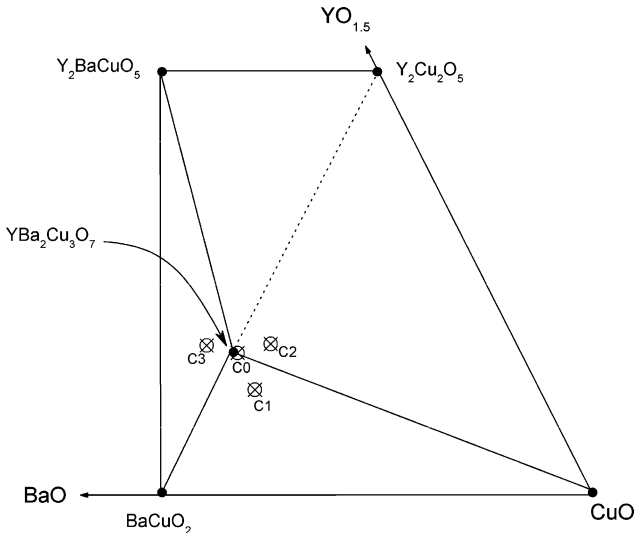

Fig. 1 Locations of powder chemical compositions in the $YO_{1.5}$-BaO-CuO equilibrium diagram

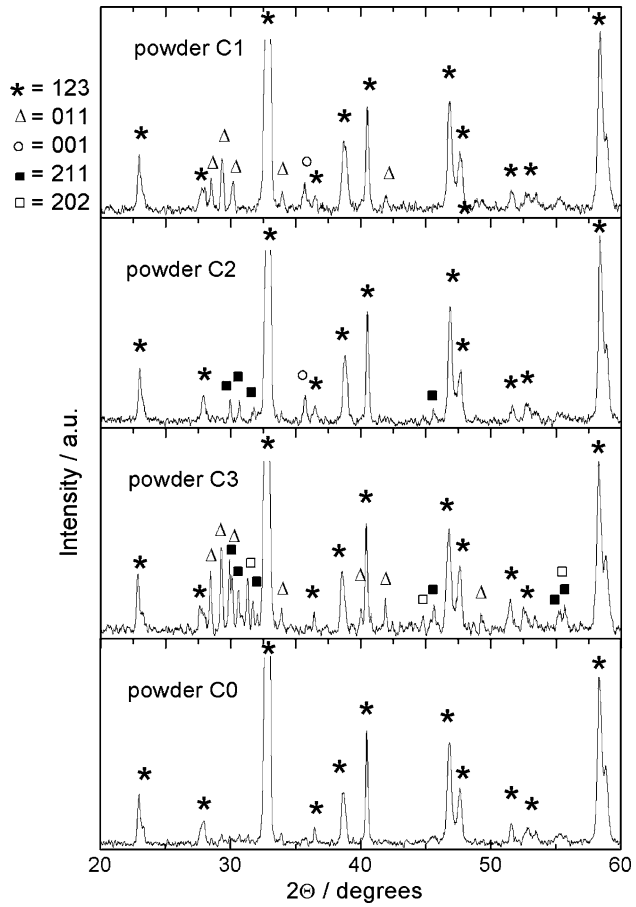

Fig. 2 X-rays diffraction patterns of calcined powders

Table 2 Crystal phases found in C1, C2, C3, and C0 after treatment at 890 °C (12 h, O_2)

Powder	Crystalline phases
C1	$YBa_2Cu_3O_7$; $BaCuO_2$; CuO
C2	$YBa_2Cu_3O_7$; Y_2BaCuO_5; CuO
C3	$YBa_2Cu_3O_7$; $BaCuO_2$; Y_2BaCuO_5; $Y_2Cu_2O_5$
C0	$YBa_2Cu_3O_7$

phases are: (123) = $YBa_2Cu_3O_7$, (001) = CuO, (011) = $BaCuO_2$, (211) = Y_2BaCuO_5, (202) = $Y_2Cu_2O_5$.

The main phase found for every specimen was 123, and the secondary phases detected depended, as expected, strongly on the individual compositions.

Reactions during heating

In Fig. 3 the DTA-TG traces of powders pre-heated at 890 °C in O_2 are shown. A well-defined peritectic melting peak (Tp) was obtained only for C0 and the composition deficient in copper oxide C3. Besides, for C0 only one peak at 971 °C was found in the range T < Tp.

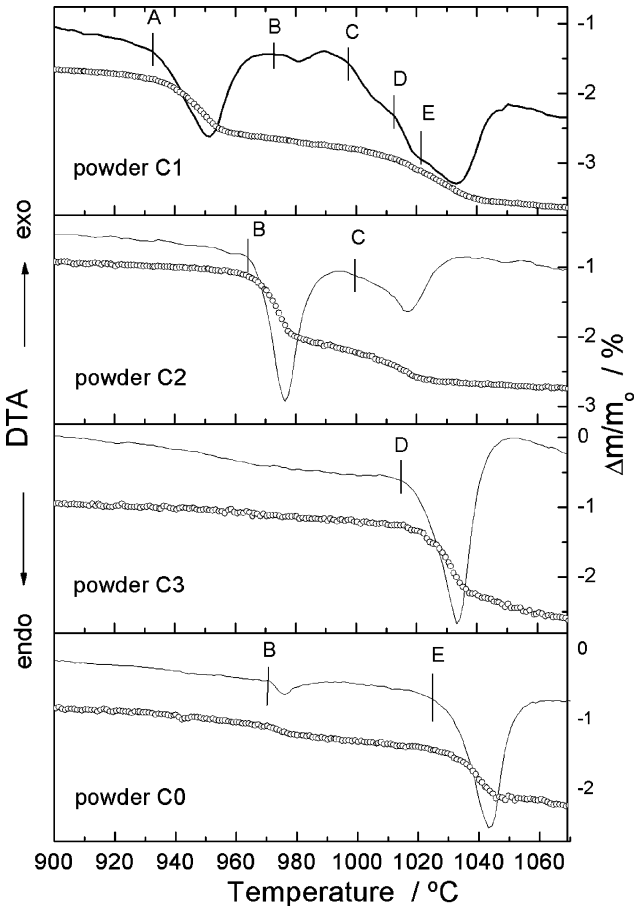

Fig. 3 DTA and TG curves (10 °C min^{-1} under O_2 flow) of calcined powders

The endothermic reactions for temperatures lower than about 1,028 °C are analyzed following the works in references [12–14]. The reactions were identified as eutectics (e_x), pseudo-peritectics or equilibrium between four phases (p_x) and peritectics or incongruent melts (m_x).The first endothermic peak (A: 925–935 °C) is assigned to the following reactants and products:

$$YBa_2Cu_3O_{7-x} + BaCuO_2 + CuO \rightarrow L(e1) \quad (1a)$$

$$BaCuO_2 + CuO \rightarrow L(e2) \quad (1b)$$

Reaction (1a) is probably present in composition C1 since—after the treatment at 890 °C—it showed phases 001 and 011 as well as the main 123 phase (Table 2). From the data for C1 it was obtained in [4] the enthalpy (ΔH) of reaction (1a), being $\Delta H_{e1} = 353$ kJ/kg, valid for $pO_2 = 0.098$ MPa. The molar composition of L(e1) is $1.25YO_{1.5} \cdot 28.75BaO \cdot 70CuO$ [15].

The second peak (B: 963–971 °C) may be assigned to reaction (2) and it was observed in compositions C1 and C2 for which CuO was clearly detected.

$$2(YBa_2Cu_3O_{7-x}) + CuO \rightarrow Y_2BaCuO_5 + L(p1) \quad (2)$$

In this reaction, the composition (mole %) of L(p1) is $3.7YO_{1.5} \cdot 22.3BaO \cdot 74CuO$ [15]. For C1 it is difficult to assign a definite value for $\Delta m/m_o$ at around 970 °C although a small jump may be detected in Fig. 3. Following the calculation procedure in [4] based in the DTA-TG data for composition C2, an enthalpy of reaction (5): $\Delta H_{p1} = 293$ kJ/kg was obtained.

A possible third peak (C: 995–1,005 °C) may be attributed to reaction (3):

$$Y_2BaCuO_5 + CuO \rightarrow Y_2Cu_2O_5 + L(p2). \quad (3)$$

From [15], the composition (mole %) of L(p2) is $4YO_{1.5} \cdot 20BaO \cdot 76CuO$. This peak C is detected in C2 and may be justified by the presence of phases 211 and 001 in the powder (Fig. 2) before the DTA-TG runs. For C1 this peak is also found although the 211 phase was not detected by XRD (Fig. 2 and Table 2). However, the needed 211 may have come from reaction (3), which also occurred for such composition C1 at 970 °C. Thus, process (3) may also explain the presence of the C-peak for C1.

A fourth peak (D: 1012–1015 °C) prior to the peritectic decomposition of 123 could be related to the reactions (4a, 4b, 4c) listed in [12].

$$2(YBa_2Cu_3O_{7-x}) + BaCuO_2 \rightarrow Y_2BaCuO_5 + L(p3) \quad (4a)$$

$$BaCuO_2 \rightarrow L(m2) \quad (4b)$$

$$Y_2BaCuO_5 + BaCuO_2 \rightarrow L(e3) \quad (4c)$$

The small D-peak (or jump) for C1 and C3 corresponding to the melting of 011 phase, according to reaction (4b), would be expected because that phase was found in both compositions (see Fig. 2 and Table 2).

According to the analysis in [14], reactions (4a) and (4c) involve only a small quantity of yttrium and this would mean low consumptions of 123 and 211 in these reactions.

Krabbes et al. [15] obtained the liquid L(p3) containing $0.4\%YO_{1.5}$ (mole% = $0.4YO_{1.5} \cdot 49.2BaO \cdot 50.4CuO$) and the yttrium-free liquid L(m2) (mole% = $50BaO \cdot 50CuO$). Also, from the equilibrium diagram quoted by Aselage and Keefer [14] it may be noted that the positions for (e3) and (p3) are very close to the position for (m2) associated to the melting of the 011 phase. It can then be said that the three liquids L(p3), L(e3) and L(m2) have roughly similar compositions and they are obtained at more or less similar temperatures. The changes in $\Delta m/m_o$ for C1 and C3 for peak D cannot be separated from that for the decomposition/melting of 123 owing to the similar temperatures.

The peritectic melting reaction (E: 1,020–1,035 °C) for the tetragonal 123 phase may be represented by reaction (5):

$$2(YBa_2Cu_3O_{7-x}) \rightarrow Y_2BaCuO_5 + L(m1) \quad (5)$$

This reaction (5) is clearly noted for compositions C0 and C3, whereas for compositions C1 and C2 this reaction

is probably masked by the preceding reactions (3) and (4a, 4b, 4c). Considering that the molar composition of L(m1) is $4YO_{1.5}$. 36.5BaO. 59.5CuO [15], the enthalpy of reaction (5), under pure O_2 atmosphere, was calculated from the DTA-TG data of C0 [4]: $\Delta H_{m1} = 143$ kJ/kg.

To understand the high temperature thermodynamic behavior of the $YO_{1.5}$-BaO-CuO system the enthalpies of reactions (1a), (2) and (5) are of great importance. As noted above, these values were estimated from dynamic DTA-TG measurements. To our knowledge such calorimetric estimations of heat of reactions for this system are not available in the literature. Furthermore, the present value for ΔH_{m1} of 143 $kJkg^{-1}$ (pure O_2) appears to be consistent with the information in [16] and previous publications of that group.

Densification behavior

In Fig. 4 are shown the dilatometric curves measured for pre-fired (750 °C) pellets of the four powders. Compact C0 gave a sintering curve very close to that for commercial powder SSC (Seattle Specialty Ceramics, Inc.) (see Fig. 2, in ref. [8]). Powder C0 only differed slightly from SSC in the DTA-TG behavior, which may be associated to the slightly higher Cu content for C0 [4].

As it is noted in Fig. 4 compacts C2 and C3 show a strong increase in ΔL/Lo after they reached densifications of around 25–28%. Such behavior corresponds to a kind of collapse of the pellets owing to the exudation of the peritectic liquids.

Compact C1 starts densification under oxygen flow at 827 °C. Applying sintering models to estimate the activation enthalpy of the dominating mechanism in each T-range it is proposed that about 85% of the total densification of C1 is related to densification under the action of a liquid phase. Details of the sintering activation energies calculated [4] upon application of different densification models will be presented in another work.

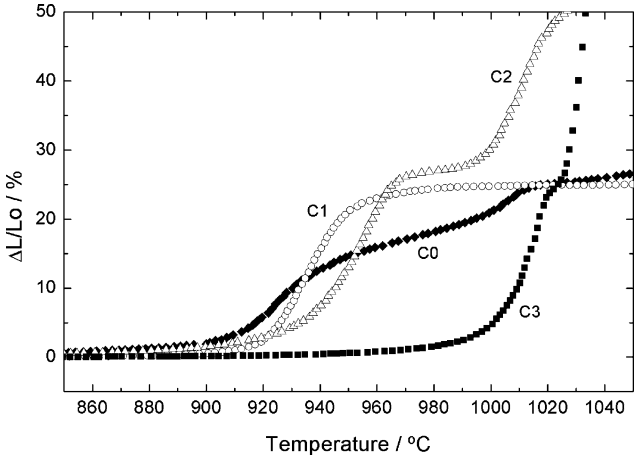

Fig. 4 Percentual absolute linear densification for compacts C0, C1, C2 and C3

This agrees with the work by Hwang et. al [17] where 123 specimens, rich in CuO, exhibited a high densification which was attributed to the presence of a liquid phase.

In the present case the existence of a liquid phase is assigned to the eutectic reaction (1a), which is obtained at 925–935 °C generating the liquid L(e1), rich in Ba and Cu. This reaction for C1 has a mass loss of oxygen of about 0.71% (pure O_2) whereas the loss for the stoichiometric L(e1) is 3.41% in air [15]. This allows to approximately estimate the amount of liquid as 21% of the initial mass of C1, and therefore, it would be expected significant densification via the rearrangement stage associated to a liquid phase sintering mechanism.

From Fig. 3, for T > 980 °C several endothermic reactions are met in powder C1, but the contraction for compact C1 remained constant (at $\Delta L/Lo \cong 24$–25%) from 980 °C up to 1,060 °C. Therefore, as no further densification is observed it can be inferred that the liquids/solids, associated to those DTA reactions, do not present any LPS- or SSS-mechanism acting in composition C1.

For compact C2 the highest shrinkage rates are found in the following T-ranges: 950–960 °C and 1,005–1,020 °C. The densification rate increases significantly from about 935 °C up to 960 °C, to decrease, then, to low values between 960 °C and 1,000 °C. For the latter range, the densification remained roughly constant with values in between 23 and 27%.

The next range from 1,005 °C to 1,060 °C does not correspond to densification processes. The detected contraction (reaching values higher than 50%) is associated to the peritectic melting/decomposition of C2 as judged from the aspect of the pellet after the whole dilatometric run; the final pellet was surrounded by the expelled peritectic liquid.

The small densification obtained for C2 from about 955 °C to 990 °C can be assigned to a weak solution-precipitation mechanism provoked by L(p1). This fact could be associated to either the solubility of 123 and/or the diffusivity of the limiting species in the liquid L(p1) are arrested for composition C2. According to the compositions of the liquids that can be formed in the $YO_{1.5}$-BaO-CuO system [18], none of them accepts more than 4 mole%$YO_{1.5}$, which is the $YO_{1.5}$ content of L(m1). For instance L(p1) contains three times more $YO_{1.5}$ than L(e1) and a little less $YO_{1.5}$ than L(m1). Then, dissolution of 123 in L(p1) would be more difficult than in L(e1) which would support the liquid phase mechanism is effectively acting in composition C1.

As it was noted above the increase in ΔL/Lo at 1,000 °C (Fig. 4) after C2 reached a densification of around 27% is assigned to exudation of the peritectic liquid. Contraction

levels higher than about 30% cannot be related to densification processes, because the density of the pellet would reach values higher than the theoretical density of the ceramic. After the exudation, C2 was found to be expanded in the radial direction and surrounded by the generated liquid. The liquid L(p2) has 4 mole% $YO_{1.5}$ and thus would not accept more yttrium [15, 19]. As a result it could not dissolve either the 123 particles or the expected 211 phase [after reaction (2)]. In this way, due to the likely low viscosity of L(p2) at this high temperature, it flowed easily out of the pellet.

For compact C3, at temperatures lower than 1,016 °C, it can only be detected a kind of very shallow wide endothermic deviation of the base line of the DTA curve (Fig. 3). The DTA trace showed a well-defined endothermic peak E between 1,016 and ~ 1,035 °C, associated with a mass loss (Δm/mo) of 1.0%. The TG losses during the peritectic reaction (5) for C0 (compositions very close to 123) was around 0.7% under O_2-flow. The increased O_2 mass losses for powder C3 may indicate that other reactions are acting during such endothermic process. For instance, for reactions (4a) and (4b) Krabbes et al. [15] found, in air atmosphere, Δm/mo losses of O_2 of 2.040% and 2.145% respectively. In [15] it is also reported reaction (p4): 211 + 202 → 200 + L (at about 1,061 °C in air) with Δm/mo of 1.765%. Also, in [20] it has been proposed that reactions (4a, 4b, 4c) can act as "activators" for the peritectic decomposition for compositions close to 123.

As it may be noted in the shrinkage curve for C3, for the range 1,016–1,035 °C the pellet decreased nearly 50% in height, twice as much as that detected for C2. This indicates C3 has nearly melted completely. Then, apart from reactions (4a) and (4b) it is probable that other processes like reactions (4c) and (p4; [15]) could have happened in this composition C3.

The small densification from 904 °C up to 976 °C appears to be consistent with the results in [21], where for Cu(y) levels ($2.80 \leq y \leq 3.00$) no microstructural/densification evidence was obtained up to about 950 °C in air (equivalent to 970 °C in oxygen) in the $YBa_2Cu_yO_x$ system.

Conclusions

As concluding remarks it is stressed that relatively small compositional changes around 123 provoke very important differences in the endothermic reactions. Such reactions could be identified and the enthalpies of most of them could be calculated giving reasonable values. Such values are important in modelling the type of liquids generated in the 123 system as function of the chemical composition and the partial pressure of O_2.

The adopted sol–gel method permitted the final chemical compositions to be easily varied. As it was noted in the introduction, several compositions shifted from 123 can be very relevant to the growth of 123 in plate form on $SrTiO_3$ ceramic substrates.

Then, and depending strongly on composition, it is found that, for higher temperatures, the ceramics rich in copper oxide can sinter very strongly through the liquid phase process. This is particularly valid when the generated liquid can dissolve 123 and this appears to be related very strongly to the yttrium content of such liquid. From inspection of the densification/melting curves for temperatures near the peritectic point, it is clear that certain compositions do not sustain a normal peritectic decomposition, but that they rather collapse or melt to a large extent. This fact makes it very difficult to consider such ceramics for the oriented growth in plate form, useful to attain high critical currents of 123 during solidification cycles.

Acknowledgements The authors thank to Mr. Sergio Ribeiro for the NAA measurements, to Mr. Carlos Cotaro and Mrs. Silvia Dútrus for the SEM/EDAX imaging and measurements, and, to Mr. Daniel Quattrini for the DTA/TG measurements. It is acknowledged the financial support of the Centro Atómico Bariloche Superconductivity Group, which allowed the purchase of the main parts of the dilatometer. It is thank the critical reading of this work by Dr. J. M. Rincón of Instituto E. Torroja (Madrid, Spain).

References

1. Cheng CW, Rosse-Innes AC, Alford McN, Harmer MA, Birchall JD. The effect of porosity on the superconducting properties of $YBa_2Cu_3O_x$ ceramics. Supercond. Sci Technol. 1988;1:113–7.
2. Clarke DR, Shaw TM, Dimos D. Issues in the processing of cuprate ceramic superconductors. J Am Ceram Soc. 1989;72:1103–13.
3. Shaw TM, Dimos D, Batson PE, Schrott AG, Clarke DR, Duncombe PR. Carbon retention in $YBa_2Cu_3O_{7-d}$ and its effect on the superconducting transition. J Mater Res. 1990;5:1176–84.
4. ER Benavidez. High temperature behaviour of thin films, thick layers, powders and compacts in the $YBa_2Cu_3O_{7-x}$ superconductor system. PhD Thesis. Rosario, Argentina:Universidad Nacional de Rosario;2001
5. Karppinen M, Niinistö L, Yamauchi H. Studies on the oxygen stoichiometry in superconducting cuprates by thermoanalytical methods. J Thermal Anal. 1997;48:1123–41.
6. Nenartaviciene G, Nsuaadu T, Jasaitis D, Beganskiene A, Kareiva A. Preparation and characterization of superconducting $YBa_2(-Cu_{1-x}Cr_x)_4O_8$ oxides by thermal analysis. J Therm Anal. 2007;90:173–8.
7. Benavidez E, González Oliver CJR, Caruso R, de Sanctis O. Chemical method to prepare $YBa_2Cu_3O_{7-x}$ (YBCO) films by dipping onto $SrTi(Nb)O_3$ ceramics. Mater Chem Phys. 2000;62:9–17.
8. Benavidez E, González Oliver CJR. Sintering mechanisms in $YBa_2Cu_3O_{7-x}$ superconducting ceramics. J Mater Sci. 2005;40:3749–58.

9. Fiscina JE, González Oliver CJR, Esparza D. The sintering kinetics of Ag-$Y_1Ba_2Cu_3O_{7-\delta}$ laminates and the interfacial metal-ceramic reaction. Appl Superconduct. 1995;3:277–87.
10. Benavidez ER, de Sanctis O, Fiscina JE, González Oliver CJR. Densification and decomposition of $YBa_2Cu_3O_{7-y}$ ceramic, and Ag-$YBa_2Cu_3O_{7-y}$ cermet compositions in the peritectic range. J Mat Sci Lett. 2000;19:307–10.
11. Oliber EA, Benavidez ER, Requena G, Fiscina JE, González Oliver CJR. High temperature reactions, densification and the peritectic decomposition of $YBa_{2-x}Sr_xCu_3O_{7-\delta}$ (YBSCO) superconducting ceramics. Phys C. 2003;384:247–57.
12. Ullmann JE, McCallum RW, Verhoeven JD. Effect of atmosphere and rare earth on liquidus relations in the RE-Ba-Cu oxides. J Mater Res. 1989;4:752–4.
13. Lay KW, Renlund GM. Oxygen pressure effect on the Y_2O_3-BaO-CuO liquidus. J Am Ceram Soc. 1990;73:1208–13.
14. Aselage T, Keefer K. Liquidus relations in Y-Ba-Cu oxides. J Mater Res. 1988;3:1279–91.
15. Krabbes G, Wiesner U, Bieger W, Ritschel M. Oxygen balance considerations of the univariant reactions in the Y-Ba-Cu-O system at 0.21 x 10^5 Pa oxygen pressure. Z Metallkd. 1994;85:70–2.
16. Moiseev G, Vatolin N, Stepanek B, Sestak J. Estimation of melting (decomposition) of some compounds in the Y-Ba-Cu-O system. J Therm Anal. 1995;43:477–88.
17. Hwang NM, Park YK, Lee HK, Hahn JH, Bahng GW, Lee KW, Moon HG, Park JC. Effects of a liquid phase in the Y-Ba-Cu-O superconductor. J Am Ceram Soc. 1988;71:C210–1.
18. Krabbes G, Bieger W, Wiesner U, Ritschel M, Teresiak A. Isothermal sections and primary cristallization in the quasiternary $YO_{1.5}$-BaO-CuO_x system at $p(O_2) = 0.21 \times 10^5$ Pa. J Solid State Chem. 1993;103:420–32.
19. Karen P, Kjekshus A. Phase diagrams for the $YBa_2Cu_3O_7$ family-anno 1996. J Thermal Anal. 1997;48:1143–227.
20. Fiscina JE. Study and development of cermet superconductor Ag-$YBa_2Cu_3O_{7-\delta}$ system. PhD Thesis. Bariloche, Argentina:Instituto Balseiro, Universidad Nacional de Cuyo;1994.
21. Yang N, Kung JH, Wu PT. High Tc superconductivity and microstructural control of Y-Ba-Cu-O by copper stoichiometry. J Cryst Growth. 1988;91:439–43.